

Exploring Uncertainty Measures for Image-Caption Embedding-and-Retrieval Task

Kenta Hama*
hamaken@ai.cs.kobe-u.ac.jp
Kobe University
Kobe, Japan

Kuniaki Uehara
uehara@kobe-u.ac.jp
Kobe University
Kobe, Japan

Takashi Matsubara*
matsubara@phoenix.kobe-u.ac.jp
Kobe University
Kobe, Japan

Jianfei Cai
ASJFCai@ntu.edu.sg
Nanyang Technological University
Singapore

ABSTRACT

With the wide development of black-box machine learning algorithms, particularly deep neural network (DNN), the practical demand for the reliability assessment is rapidly rising. On the basis of the concept that “Bayesian deep learning knows what it does not know,” the uncertainty of DNN outputs has been investigated as a reliability measure for the classification and regression tasks. However, in the image-caption retrieval task, well-known samples are not always easy-to-retrieve samples. This study investigates two aspects of image-caption embedding-and-retrieval systems. On one hand, we quantify feature uncertainty by considering image-caption embedding as a regression task, and use it for model averaging, which can improve the retrieval performance. On the other hand, we further quantify posterior uncertainty by considering the retrieval as a classification task, and use it as a reliability measure, which can greatly improve the retrieval performance by rejecting uncertain queries. The consistent performance of two uncertainty measures is observed with different datasets (MS COCO and Flickr30k), different deep learning architectures (dropout and batch normalization), and different similarity functions.

CCS CONCEPTS

• **Computing methodologies** → *Knowledge representation and reasoning*.

KEYWORDS

uncertainty quantification, Bayesian deep learning, semantic embedding, image-caption retrieval

ACM Reference Format:

Kenta Hama, Takashi Matsubara, Kuniaki Uehara, and Jianfei Cai. 2018. Exploring Uncertainty Measures for Image-Caption Embedding-and-Retrieval

*Both authors contributed equally to this research.

Permission to make digital or hard copies of all or part of this work for personal or classroom use is granted without fee provided that copies are not made or distributed for profit or commercial advantage and that copies bear this notice and the full citation on the first page. Copyrights for components of this work owned by others than the author(s) must be honored. Abstracting with credit is permitted. To copy otherwise, to republish, to post on servers or to redistribute to lists, requires prior specific permission and/or a fee. Request permissions from permissions@acm.org.

Woodstock '18, June 03–05, 2018, Woodstock, NY

© 2018 Copyright held by the owner/author(s). Publication rights licensed to ACM.

ACM ISBN 978-1-4503-9999-9/18/06...\$15.00

<https://doi.org/10.1145/1122445.1122456>

Task. In *Woodstock '18: ACM Symposium on Neural Gaze Detection*, June 03–05, 2018, Woodstock, NY. ACM, New York, NY, USA, 10 pages. <https://doi.org/10.1145/1122445.1122456>

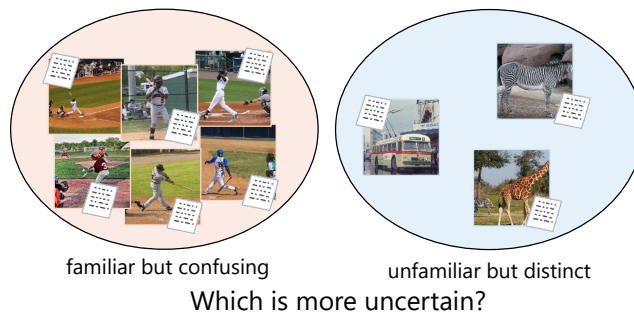


Figure 1: Conceptual diagram of uncertainty in image-caption embedding-and-retrieval task.

1 INTRODUCTION

Recent advances in machine learning algorithms have enabled us to recognize and utilize various data modalities such as vision, natural language, and sound. These algorithms, especially deep neural networks (DNNs), build black-box functions to make decisions in a data-driven manner. While their accuracy is sufficient for many real-life applications, they have encountered safety issues, e.g., self-driving systems have injured pedestrians. In addition to physical accidents, image-tagging systems and recommendation systems have also offended users by inappropriate suggestions. These issues can be caused by insufficient training samples, dataset bias, and dataset shift [21, 27, 34, 49]. With a proper reliability assessment of their decisions, the applications can reduce the number of wrong decisions and ask for human intervention. In this study, we quantify the uncertainty of image-caption embedding-and-retrieval systems as a first step toward assessing their reliability, as shown in Fig. 1.

Several studies explicitly inferred a posterior distribution of a target instead of its point estimate and regarded the posterior entropy as aleatoric uncertainty [21, 26, 31]. The aleatoric uncertainty is expected to have a large value if a given sample is ambiguous and difficult to make a decision on. However, a DNN classifier trained to minimize the empirical risk often outputs a posterior with almost

zero entropy not depending on its reliability [15, 36]. Moreover, recent state-of-the-art approaches have employed regularized training objectives [33, 41, 47], in which case, they no longer estimate true posteriors nor assess uncertainty.

Other approaches are based on Bayesian neural networks (BNNs) [2, 5, 17, 30], in which the parameters are defined as random variables. The output depends on a parameter (i.e., a model) drawn from its posterior. The output averaged over these drawn models is often more accurate than a single output; this approach is called model averaging. The variance of the output is expected to serve as an uncertainty measure called epistemic uncertainty [26]. Many recent DNNs can be BNNs because they employ stochastic components such as dropout [39] and batch normalization [18] in the training phase. When these components are also used in the inference phase, they provide a different parameter and output for each run [1, 11]. The epistemic uncertainty has been investigated for the classification task (including the segmentation task) [11, 21, 22, 27, 44] and the regression task [11, 21, 44], and has successfully detected misclassifications and excessive errors. However, it still remains unclear how to define the epistemic uncertainty for other tasks such as the semantic embedding task.

This study focuses on the uncertainty from the two aspects of image-caption embedding-and-retrieval systems [9, 10, 13, 20, 25, 43, 48]. The embedding task can be regarded as a regression task because its purpose is to arrange given samples in an embedded space [40]. However, the performance of embedding has often been evaluated by the retrieval task, which is very similar to the classification task [6, 19, 48].

Contributions. This study explores uncertainty measures for the embedding-and-retrieval task. We demonstrate that the embedding-and-retrieval task can be regarded as a regression task and a classification task and that one has to evaluate an embedding-and-retrieval system in these aspects. Section 3 proposes a new approach to estimate the posterior distributions that a given query is associated with a target sample even though the objective function is the rank loss [9, 10, 20, 25, 43, 48]. Then, we propose feature and posterior uncertainties from viewpoints of regression and classification tasks, respectively. In Section 4, we demonstrate that, for improving the performance of the retrieval task, model averaging based on these two uncertainties works similarly well. For assessing the reliability, the posterior uncertainty provides a better reliability measure for the retrieval task than the feature uncertainty. These tendencies are common for different datasets, DNN architectures, and similarity functions. Also, the posterior uncertainty quantifies the dataset shift, whereas the feature uncertainty cannot do this. A qualitative comparison of these uncertainties reveals that the tendencies are caused by the biases in multi-modal datasets; a dataset containing many similar samples makes the DNN familiar with and certain about these samples, but the same dataset provides the confusing task of retrieving a desired sample from many similar samples, as exemplified in Fig. 1. All results are based on the MS COCO [29], Flickr30k [46], and RecipeQA [45] datasets.

2 RELATED WORKS

2.1 Bayesian Neural Networks

A typical DNN is a map from an input x to an output y parameterized by w , which is expressed as $y = DNN(x, w)$, hereafter. Given a dataset $D = \{(x_i, t_i)\}_{i=1}^N$ for a classification task, the target t_i is the class to which the input x_i belongs, and the output y_i is typically an estimate of its posterior probability $y_i = p(t_i|x_i, w)$. For a regression task, the output y_i is a point estimate of the target t_i or its posterior distribution $p(t_i|x_i, w)$, expressed using the reparameterization trick [21, 22, 24].

A BNN is a neural network whose parameter w is estimated as a posterior distribution $p(w|D)$ given a dataset D . Because the true posterior $p(w|D)$ is intractable, many approximation methods have been proposed [2, 5, 17, 30]. Recent studies have revealed that the optimization of a DNN using stochastic components such as dropout [39] and batch normalization [18] provides an approximated posterior $q(w|D)$ of the parameter w [1, 11]. The original proposers supposed to average the parameter w over the approximated posterior $q(w|D)$ in the inference phase. Specifically, the output is $y = DNN(x, \bar{w})$ for $\bar{w} = \mathbb{E}_{q(w|D)}[w]$, and this approach is called *weight averaging* [21, 22]. However, one can draw a new instance of the parameter w from the posterior $q(w|D)$ even in the inference phase. Each drawn instance of the parameter w provides a single model $p(t|x, w)$. Drawing multiple models, one can obtain a more accurate posterior by averaging the posteriors as

$$\begin{aligned} y &= p(t|x, D) \\ &= \int_w p(w|D)p(t|x, w) \\ &\approx \int_w q(w|D)p(t|x, w). \end{aligned} \quad (1)$$

This approach is called *model averaging* [5, 22]. Because the integral of a DNN is intractable, the expectation over the posterior $q(w|D)$ is approximated using Monte Carlo sampling of L models. Many previous studies have confirmed that the model averaging improves the classification accuracy [1, 11, 21, 22, 44]. The regression task often employs non-probabilistic measures such as the mean squared error and L_1 distance, and the rigorous model averaging does not always improve these measures. Instead, the output y is simply averaged over the weight posterior $q(w|D)$ [11, 21, 40, 44] as

$$y = \mathbb{E}_{q(w|D)}[DNN(x, w)] \quad (2)$$

2.2 Uncertainty Quantification

In an exact Bayesian inference, the parameter w first follows a prior $p(w)$ and then is gradually specified as the number of observed samples increases. The posterior distribution $p(t|x_i, D)$ also has a large variance at the beginning and then approaches the target t_i [42]. Similarly, the BNN is trained to provide an output y_i robust to the stochastic behavior of dropout and batch normalization. Given unfamiliar inputs such as samples from a different dataset or domain, the outputs still suffer from the stochastic behavior and have large variances [21, 27]. This behavior is similar to that of a Gaussian process [11]. The output variance $Var_{q(w|D)}[y]$ is an uncertainty measure called epistemic uncertainty, and it is available for assessing the reliability of decision making. This usage is based on the

assumption that a decision on an unfamiliar sample is unreliable. For the classification task, an alternative is the mutual information $I(t; w|x, D)$ between the class posterior and the parameter w [38]. The variance of the class posterior $p(t|x, D)$ can be considered as a first-order approximation of the mutual information.

2.3 Semantic Embedding-and-Retrieval

Representation learning is one of the greatest concerns of recent machine learning studies [4]. The primary purpose of representation learning is to build a map that projects a given input to a feature that represents useful information for successive tasks. A good representation arranges the inputs following their semantic relationships, captures the underlying mechanism of the input, or contains only the information of interest without nuisance factors [3, 12, 16, 32].

Semantic embedding is a supervised representation learning task [9, 10, 13, 20, 25, 43, 48]. Its purpose is to arrange samples so that similar samples are close to each other in the embedded space. Typically, a dataset is divided into many small groups of similar samples (e.g., a group of an image and five captions [29]). Given a sample (called a query), the DNN is expected to find similar samples according to their distances in the embedded space. From this viewpoint, the semantic embedding is a regression task without identifiability. However, the performance of the semantic embedding has often been evaluated by the retrieval task, whose purpose is to find the most similar sample to the query from candidates (called targets). When regarding the given sample as a representative point of a class, the retrieval task becomes a classification task. In fact, the semantic embedding has been employed for one-shot classification and extreme multi-class classification [6, 19, 48].

3 UNCERTAINTY MEASURES FOR EMBEDDING-AND-RETRIEVAL

3.1 Feature Uncertainty for Embedding

For the semantic embedding, a DNN outputs a feature vector y given a sample x . Given a similarity ranking of samples or groups of samples, the DNN is trained to embed a sample so that it is close to similar samples in the embedded space. Specifically, the distance from a query sample x_q to a designated target x_p (called a positive target) should be closer than that to another target x_n (called a negative target). The 0-1 loss for this objective is $I(s(y_q, y_p) > s(y_q, y_n))$, where $s(\cdot, \cdot)$ is a similarity function and $I(cond)$ is the indicator function [43]. Because it is difficult to optimize the 0-1 loss, the following hinge rank loss has been widely used [9, 10, 13, 20, 25, 35, 43, 48].

$$\mathcal{L}_{emb}(x_q, x_p, x_n) = |s(y_q, y_n) - s(y_q, y_p) + m|_+, \quad (3)$$

where $|\cdot|_+$ is the positive part and $m > 0$ is a margin parameter. The similarity function $s(\cdot, \cdot)$ can be the negative Euclidean distance, inner product, or cosine similarity in the embedded space. Note that recent studies have preferred the cosine similarity, which suppresses an excessive similarity and distance [9, 13].

When the DNNs are BNNs, the similarity function $s(\cdot, \cdot)$ depends on the drawn parameter w and the hinge rank loss is averaged over the parameter posterior $q(w|D)$. The epistemic uncertainty of a sample x is defined as the variance of the feature vector y in the

embedded space, i.e.,

$$\begin{aligned} \mathcal{U}_f(x) &= \text{Var}_{q(w|D)}[y] \\ &= \text{Var}_{q(w|D)}[\text{DNN}(x, w)]. \end{aligned} \quad (4)$$

We call this uncertainty the *feature uncertainty*, hereafter, where the variance is summed over the elements in the feature vector y . We can average the embedded feature y over the parameter posterior $q(w|D)$ as the model averaging; we call this the model averaging over feature uncertainty.

3.2 Posterior Uncertainty for Retrieval

For the classification task, the DNN outputs an intermediate feature y given a sample x [11, 21, 22, 27, 33, 41, 44, 47]. Then, a fully-connected (FC) layer and the softmax function are applied to the feature y , resulting in a posterior probability $p(c_j|x)$ that the sample x belongs to the class c_j indexed by j as follows:

$$\begin{aligned} p(c_j|y, \{w_k\}) &= \text{softmax}(y, \{w_k\})_j \\ &= \frac{\exp((w_j \cdot y)/T)}{\sum_k \exp((w_k \cdot y)/T)}, \end{aligned} \quad (5)$$

where $\{w_k\}$ is the parameter of the FC layer and T is the temperature parameter. The bias term is omitted for simplicity. Given a target posterior $q(c_j|x)$, the objective function of the classification task is typically the cross-entropy loss:

$$\mathcal{L}_{cls}(x, w, \{w_k\}) = \sum_j -q(c_j|x) \log p(c_j|y, \{w_k\}). \quad (6)$$

This loss is also called the logistic loss for binary classification [35]. The mutual information $I(c; w, \{w_k\}|x, D)$ between the posterior and the parameter was proposed as the epistemic uncertainty [38], which is calculated as

$$\begin{aligned} \mathcal{U}_p(x) &= I(c; w, \{w_k\}|x, D) \\ &= H(\mathbb{E}_{q(w, \{w_k\}|D)}[p(c|x, w, \{w_k\})]) \\ &\quad - \mathbb{E}_{q(w, \{w_k\}|D)}[H(p(c|x, w, \{w_k\}))]. \end{aligned} \quad (7)$$

The mutual information can be calculated as the difference of the entropy before and after the model averaging. From another viewpoint, the mutual information is a measure of reduction in the entropy of the parameter w after the label c is given. If the DNN is already trained with samples similar to the given sample x , the parameter w is updated only a little and the mutual information is small, and vice versa. The mutual information measures how informative a new sample x and label c pair is for the DNN.

The cross-entropy loss is commonly used by embedding-and-retrieval systems of person images (i.e., person re-identification systems) [28]. These systems classify an image set of the same person as a class and use the extracted features y as the embedded features for retrieval. In contrast, this loss is much less common for multi-modal embedding-and-retrieval systems, and their results were often inferior to the results with the hinge rank loss [28, 50]. For both multi-modal retrieval system and person re-identification system, we have no weight parameter w_k for a new class in the retrieval phase. Instead, using the similarity, we assume the posterior probability that a target x_j is the best positive target of all targets $\{x_k\}$ for a query x_q in the retrieval phase as

$$p(c_j|x_q, \{x_k\}) = \frac{\exp(s(y_q, y_j)/T)}{\sum_k \exp(s(y_q, y_k)/T)}, \quad (8)$$

where the binary variable c_j has a value of 1 if x_j is the best positive target for the query x_q . The embedded feature y_k of a target x_k corresponds to the parameter w_k for the ordinary classification. Given targets $\{x_k\}$, we define the mutual information $\mathcal{U}_p(x)$ as an uncertainty called the *posterior uncertainty*, hereafter. We emphasize that, unlike the feature uncertainty, the posterior uncertainty is defined with targets unlike the feature uncertainty. We can average the retrieval posterior $p(c_j|x_q, \{x_k\})$ over the parameter posterior $q(w|D)$ using the model averaging; we call this the model averaging over posterior uncertainty. For simplicity, we average the feature vectors $\{y_k\}$ of the targets $\{x_k\}$ before calculating the retrieval posterior and evaluate the posterior uncertainty only for queries. We have empirically found that this simplification does not influence the performance and results much. In addition, we empirically confirmed that the variance of the retrieval posterior demonstrated the same tendency as that of the mutual information in all experiments as shown in [38], and hence, we omitted the results of the variance of the retrieval posterior in this paper.

Note that the similarity function $s(\cdot, \cdot)$ is not necessarily the inner product but typically the cosine similarity, which is bounded in the range $[-1, 1]$. As a result, the posterior probability is never close to 0.0 or 1.0 when $T = 1.0$.

4 EXPERIMENTS AND RESULTS

4.1 Experimental Settings

For the image-caption retrieval task, we employed the typical DNN architecture, VSE++ [9]. We used the source code provided by the original authors¹ and the original experimental settings unless otherwise stated. VSE++ has an image encoder and text encoder. For image encoding, we used VGG19 [37] pretrained using the ImageNet dataset [8]. We removed the final FC layer for classification and added a new FC layer for embedding. The dimension number of the embedded space was 1024. Dropout [39] with a keep probability $p = 0.5$ was already applied before each FC layer. We resized each input image so that the smaller edge was 256 and cropped it to a 224×224 region randomly in the training phase. In the retrieval phase, we cropped the center region. For text encoding, we used a GRU-based text encoder, which is a kind of recurrent neural network [7]. Each word was expressed as a one-hot coded vector and projected to a word embedded space using an affine transformation. The dimension number of the word embedded space was 300. Then, a GRU network read the embedded words in a sentence sequentially outputted a vector, which was used as an embedded feature. In addition to the original experimental settings, we applied dropout with a keep probability $p = 0.9$ to the word embedded space to obtain stochasticity. In the training phase, we minimized the hinge rank loss only with the closest negative target and discarded the losses with other negative targets. Specifically,

$$\mathcal{L}_{emb}(x_q, x_p, \{x_n\}) = \max_n |s(y_q, y_n) - s(y_q, y_p) + m|_+, \quad (9)$$

where $\{x_n\}$ denotes negative targets in a mini-batch and the margin m was set to 0.2. The similarity function $s(\cdot, \cdot)$ was the cosine similarity.

We evaluated VSE++ on the MS COCO [29] and Flickr30k [46] datasets using the splits used by the original VSE++ [9]. For the MS

¹<https://github.com/fartashf/vsepp>

COCO dataset, we used 113,287 images for training, 5,000 images for validation, and 5,000 images for testing. We reported the performance averaged over 5-folds of validation/testing images. For the Flickr30k dataset, we used 30,000 images for training, 1,000 images for validation, and 1,000 images for testing. Each image has five captions as positive targets.

The VGG19 and GRU network were jointly optimized for 45 epochs using the Adam optimizer [23] with a batch-size of 128. The VGG19 except for the final FC layer was frozen for the first 30 epochs and unfrozen for the remaining 15 epochs. The learning rate was initialized to 2×10^{-4} , and then, it was reduced by 0.1 at 15th and 30th epochs.

A typical performance measure of the retrieval is recall at K , which is the fraction of positive targets in the top K candidates. $R@K$ denotes the performance of caption retrieval based on an image query, and $Ri@K$ denotes that of image retrieval based on a caption query. The model was evaluated on the sum of $R@1$, $R@5$, $R@10$, $Ri@1$, $Ri@5$, and $Ri@10$ for the validation set after every epoch using the weight averaging, and the best snapshot was selected. We also reported the performance measure Med r , which is the median rank of the first positive target.

We also evaluated VSE++ with ResNet152 [14] as the image encoder. ResNet152 has no dropout but employs batch normalization. We applied the stochastic batch normalization [1] to obtain the stochasticity in the retrieval phase; the stochastic batch normalization learns the distribution of the normalization parameters of batch normalization in the training phase and draws parameters from the distribution in the retrieval phase. One can regard the ordinary batch normalization in the retrieval phase as the weight averaging.

Moreover, we evaluated VSE0 with VGG19, which employed the inner product as the similarity function and minimized the hinge rank loss averaged over all negative targets in a mini-batch [9] as follows.

$$\mathcal{L}_{emb}(x_q, x_p, \{x_n\}) = \frac{1}{|\{x_n\}|} \sum_n |s(y_q, y_n) - s(y_q, y_p) + m|_+. \quad (10)$$

This objective function was formerly used for image-caption retrieval tasks [25].

4.2 Retrieval Performance with Model Averaging

We evaluated the performance on the image-caption retrieval. First, we focus on VSE++ with VGG19. We evaluated the model averaging over feature uncertainty and over posterior uncertainty as introduced in Section 3. For the posterior uncertainty, we adjusted the temperature parameter T from 0.001, 0.01, 0.1, 1.0, and 10. As a baseline, we evaluated the weight averaging, which averages the stochastic parameters over the posterior distribution. The weight averaging is a typical way to use dropout and batch normalization in the retrieval phase. We plotted $R@1$, $Ri@1$, $R@10$, and $Ri@10$ using the MS COCO dataset with varying the number L of drawn models in Figs. 2 (a)–(d), respectively. Each result was averaged over 3 runs from scratch.

As the number L of models increases, the retrieval performances obtained with the model averaging improve and finally outperform

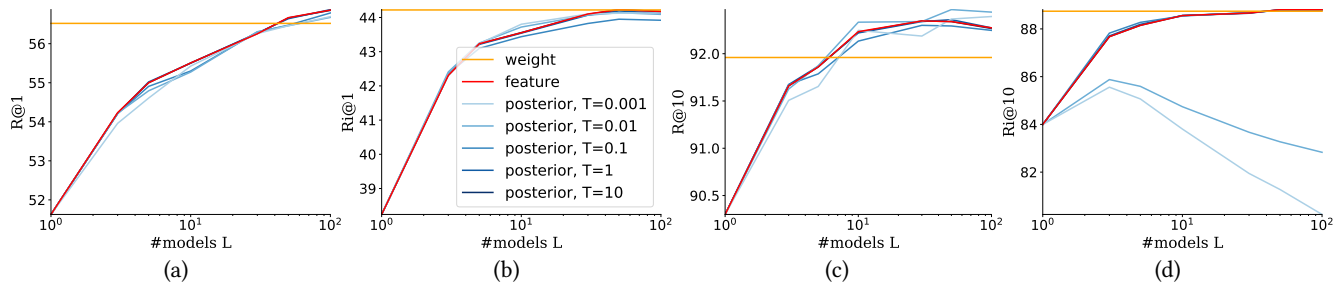


Figure 2: Retrieval performances of VSE++ with VGG19 using ms coco dataset.

Table 1: Retrieval performances

Model	Dataset			Caption Retrieval				Image Retrieval			
	Training	Testing	Averaging	R@1↑	R@5↑	R@10↑	Med r↓	Ri@1↑	Ri@5↑	Ri@10↑	Med r↓
(1) VSE++ with VGG19	MS COCO	MS COCO	weight	56.5	84.4	92.0	1.0	44.2	78.4	88.7	2.0
			feature	56.9	84.4	92.3	1.0	44.2	78.5	88.8	2.0
			posterior	56.9	84.4	92.3	1.0	44.2	78.5	88.8	2.0
(2) VSE++ with VGG19	Flickr30k	Flickr30k	weight	40.1	67.5	76.7	2.0	30.0	59.8	70.3	3.3
			feature	40.7	68.4	77.4	2.0	30.2	60.1	70.7	3.3
			posterior	40.7	68.4	77.3	2.0	30.2	60.1	70.7	3.3
(3) VSE++ with VGG19	MS COCO	Flickr30k	weight	35.0	61.8	73.1	3.0	25.9	52.2	63.6	5.0
			feature	35.8	62.6	74.0	3.0	26.1	52.3	63.9	5.0
			posterior	35.8	62.6	74.0	3.0	26.1	52.3	63.8	5.0
(4) VSE++ with ResNet	MS COCO	MS COCO	weight	65.3	90.1	96.0	1.0	50.4	83.3	91.6	1.3
			feature	64.8	89.9	95.9	1.0	50.4	83.3	91.7	1.3
			posterior	64.8	89.9	96.0	1.0	50.4	83.3	91.7	1.3
(5) VSE0 with VGG19	MS COCO	MS COCO	weight	50.2	81.5	90.6	1.3	38.3	74.6	87.0	2.0
			feature	50.4	81.5	90.5	1.4	38.8	74.8	87.1	2.0
			posterior	50.4	81.5	90.5	1.4	38.8	74.8	87.1	2.0

↑ indicates that a larger value is better and ↓ indicates that a smaller value is better.

those of the weight averaging for large L cases. This result demonstrates that the model averaging works well for image-caption retrieval, as it does for other tasks [11, 21, 22, 27, 40, 44]. The model averaging over feature uncertainty achieved the best results on average. The model averaging over posterior uncertainty $T = 10$ provided almost the same performances for any number L of models. A lower temperature improves the performance for $R@10$ and degrades it for $Ri@10$. A lower temperature leads the retrieval posterior $p(c_j|x_q, \{x_k\})$ saturated at 0.0 or 1.0, suppresses the influence of a decision with high confidence, and involves more models in the final decision. This property potentially improves the performance, but a single incorrect decision can disturb the final decision. Conversely, with a higher temperature, the retrieval posterior becomes close to linearly with the similarity, reducing the influence of a minority decision and making the final decision more robust.

The improvement of image retrieval is limited compared to that of caption retrieval. The VGG19 was designed using dropout in the original study [37] while the GRU network was not. For the model averaging, the GRU network applied the same stochastic components to a given sample repeatedly. This behavior leads to excessive variances of the intermediate features and potentially surpasses the improvement by the model averaging.

We summarized the results under other conditions in Table 1 with the number of models $L = 100$ and the temperature $T = 10$. All the results demonstrated that the model averaging yields better performances than the weight averaging, and the posterior uncertainty with the temperature $T = 10$ and the feature uncertainty are comparable. This tendency was common for different datasets (cases (1) and (2)), for dataset shift (case (3)), and for similarity functions (case (1) and (5)).

For ResNet and batch normalization (case (4)), the model averaging using $L = 100$ models did not improve the performance. We found that the model averaging is almost comparable to the weight averaging even in a single model case ($L = 1$), gradually improves the performance as L increases, and requires more than $L = 300$ models to outperform the weight averaging. The main purpose of batch normalization is to normalize the moments of intermediate activations over samples, and its stochastic behavior due to the random mini-batch selection is insufficient for obtaining diverse models.

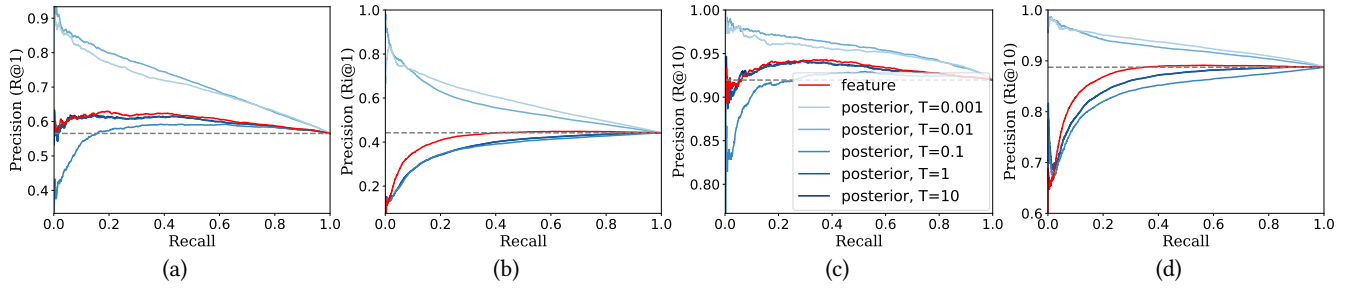


Figure 3: Precision-recall curves of VSE++ with VGG19 on ms coco dataset.

Table 2: Area under precision-recall curve (AUPRC) for reliability assessment.

Model	Dataset		Uncertainty	Caption Retrieval				Image Retrieval			
	Training	Testing		R@1↑	R@5↑	R@10↑	Med r↓	Ri@1↑	Ri@5↑	Ri@10↑	Med r↓
(1) VSE++ with VGG19	MS COCO	MS COCO	chance level	56.5	84.4	92.0	1.0	44.2	78.4	88.7	2.0
			feature	60.4	86.1	93.2	1.3	41.7	75.5	87.1	2.3
			posterior	70.4	90.3	95.2	1.0	58.6	86.0	93.1	1.2
(2) VSE++ with VGG19	Flickr30k	Flickr30k	chance level	40.1	67.5	76.7	2.0	30.0	59.8	70.3	3.3
			feature	39.1	66.9	74.9	2.9	24.5	50.9	61.7	6.8
			posterior	55.5	78.8	85.8	1.3	44.2	71.9	80.3	2.1
(3) VSE++ with VGG19	MS COCO	Flickr30k	chance level	35.0	61.8	73.1	3.0	25.9	52.2	63.6	5.0
			feature	40.2	67.9	78.8	2.4	26.2	52.4	64.1	5.1
			posterior	50.4	72.4	81.8	1.7	39.4	63.8	73.0	2.8
(4) VSE++ with ResNet	MS COCO	MS COCO	chance level	65.3	90.1	96.0	1.0	50.4	83.3	91.6	1.9
			feature	71.6	93.5	97.7	1.0	50.1	82.4	91.1	1.9
			posterior	75.1	93.3	97.4	1.0	65.7	90.0	95.3	1.0
(5) VSE0 with VGG19	MS COCO	MS COCO	chance level	50.2	81.5	90.6	1.3	38.3	74.6	87.0	2.0
			feature	49.3	81.5	91.1	1.6	34.6	72.9	87.0	2.4
			posterior	63.2	88.0	94.3	1.0	50.4	81.8	91.3	1.5

↑ indicates that a larger value is better and ↓ indicates that a smaller value is better.

4.3 Reliability Assessment of Image-Caption Retrieval

We evaluated the relationships between the uncertainty measures and the reliability of the outputs. A query with a high uncertainty is considered unreliable and tends to lead to mis-retrieval. Hence, the performance can be improved by rejecting uncertain queries. There is a trade-off between the fraction of remaining queries (recall) and the performance (precision). Hence, we report the precision-recall (PR) curves obtained by varying the rejection threshold [21]. When an uncertainty measure captures the reliability of retrieval results well, the area under the PR curve (AUPRC) is large. We evaluated VSE++ with VGG19 using the MS COCO dataset and show the PR curves of R@1, Ri@1, R@10, and Ri@10 in Figs. 3 (a)–(d), respectively. For fair comparison, the performances were obtained using the weight averaging. The dotted lines denote the chance levels, where queries are rejected randomly and the precision is unchanged from the case with recall= 1.0.

As the temperature T decreases, the PR curves obtained from the posterior uncertainty move outward, and the posterior uncertainty with the lowest temperature $T = 0.001$ yields the largest AUPRC in

most cases. The posterior uncertainty works well for the reliability assessment of retrieval.

The feature uncertainty yields PR curves lying slightly above the horizontal axes at recall > 0.5 and rapidly decreasing at a small recall, indicating that VSE++ failed in finding positive targets for queries with small feature uncertainties. The performance of the feature uncertainty for the reliability assessment is at chance levels or only slightly better than them.

At a higher value of the temperature T , the retrieval posterior $p(c_j|x_q, \{x_k\})$ becomes flatter, and any queries and targets are informative; the signal-to-noise ratio of the mutual information is limited. The same goes for the feature uncertainty; even if queries fluctuate in the embedded space, some of them were always close to their positive targets. Conversely, at low temperature values, the retrieval posterior $p(c_j|x_q, \{x_k\})$ is saturated at 0.0 or 1.0 and stable with respect to drawn models (i.e., the mutual information is always low) if a query is always close to its targets. The mutual information is high only when a query and its targets are truly informative and change the parameter w drastically, that is, the case close to mis-retrieval. Hence, the posterior uncertainty with a

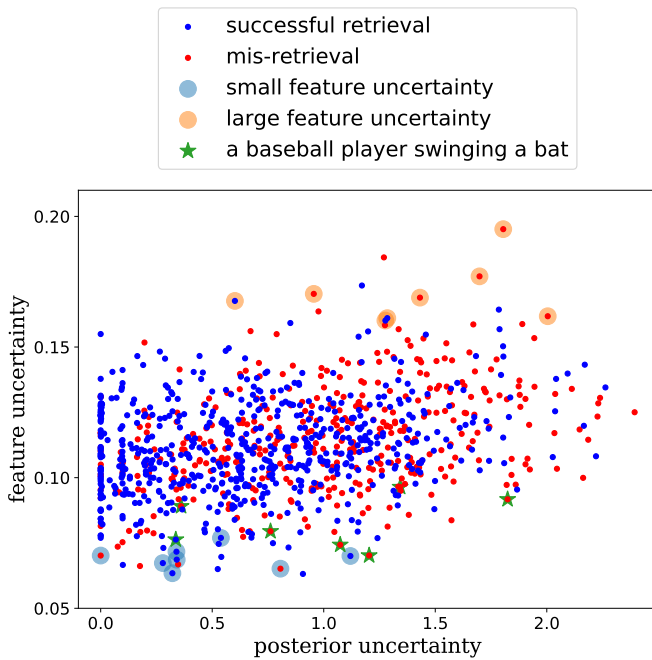


Figure 4: Scatter plot of uncertainty values for successful and failed caption retrievals on the ms coco dataset.

low temperature is the best measure of the reliability of the retrieval task.

We summarized the results under other conditions in Table 2 with the number of models $L = 100$ and the temperature $T = 0.001$. The results demonstrate that the posterior uncertainty with the temperature $T = 0.001$ worked well as a measure of reliability assessment for all cases; different datasets (cases (1) and (2)), dataset shift (case (3)), different models and stochasticity sources (cases (1) and (4)), and different similarity functions (cases (1) and (5)). In particular, the posterior uncertainty also provides a reliability measure for ResNet with batch normalization (case (4)); here, the stochastic behavior of batch normalization is sufficient for assessing reliability while being insufficient for the model averaging. The feature uncertainty was successful only for caption retrieval in cases (1), (3) and (4), and even then its performances were inferior to the posterior uncertainty. Moreover, the performance is often worse than a chance level.

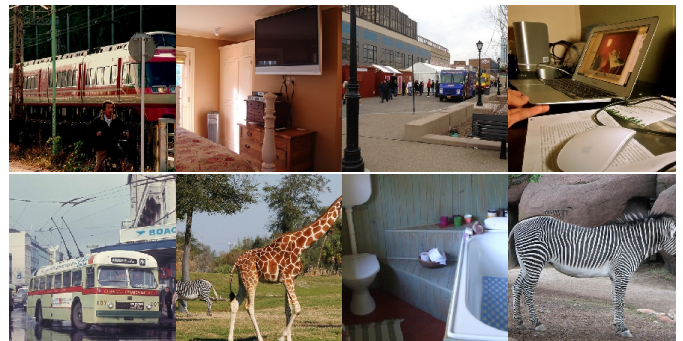
4.4 Qualitative Exploration of Large or Small Uncertainties

For a more detailed comparison of the feature uncertainty and the posterior uncertainty, we plotted the uncertainties of images in MS COCO test set in Fig. 4. The horizontal axis indicates the posterior uncertainty with the temperature $T = 0.001$ and the vertical axis indicates the feature uncertainty. We also collected example images with large or small feature uncertainties in Fig. 5. Their uncertainty values are denoted in Fig. 4.

In Fig. 5 (a), example images with small feature uncertainties tend to depict sport players or single objects in close-shots. In Fig. 5



(a) images of small feature uncertainty



(b) images of large feature uncertainty



(c) images depicting a baseball player swinging a bat

Figure 5: Example images with small feature uncertainty and large feature uncertainty, and images of a baseball player swinging a bat.

(b), example images with large feature uncertainties tend to depict animals or many objects in long-shots. This result makes sense because previous studies have demonstrated that the feature uncertainty is large for samples appearing less frequently in the training set [1, 11]. According to the annotations for object detection, more than 50 % of the training images depict people and 20 % are related to sports; the MS COCO dataset is biased to images of people and sports, and the feature uncertainty becomes small for these images. When an image depicts many objects, the DNN is likely to be unfamiliar with some of the objects, resulting in a large feature uncertainty. The feature uncertainty successfully captured the biases

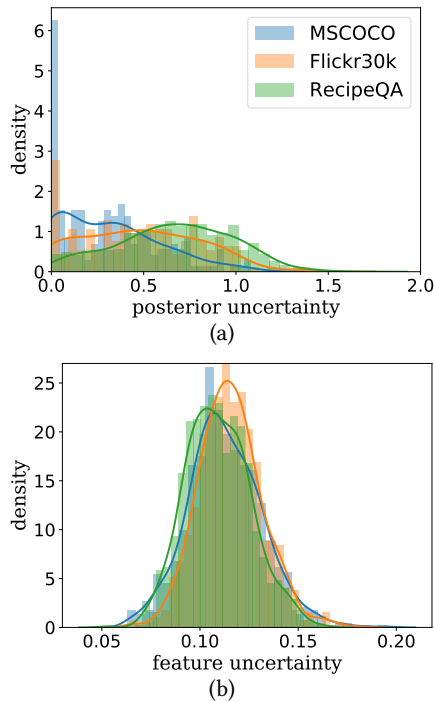


Figure 6: Distributions of uncertainty measures for caption retrieval under dataset shift.

in the dataset. However, the feature uncertainty did not evaluate the retrieval performances.

We provide a typical case showing the difference between the feature uncertainty and posterior uncertainty in Fig. 5 (c). The DNN assigns a small feature uncertainty to images depicting a baseball player swinging a bat. This is because the DNN was trained with many similar samples; according to captions, more than 1 % of the training samples are related to “baseball” and “swing”. However, given such a query, the DNN encounters the confusing task of retrieving the best target from many similar targets, and the risk of mis-retrieval increases. The posterior uncertainty captures this confusion and assigns small or large values by comparing queries with targets (see Fig. 4). Conversely, queries about animals and scenery have a limited number of similar queries and relatively distinct from each other. The DNN discriminates them from each other easily and assigns a small posterior uncertainty even though it is unfamiliar with them and assigns a high feature uncertainty. The actual reliability of retrieval depends on the relationships with targets more than the population of similar queries, and the posterior uncertainty is suited for the reliability assessment of image-caption retrieval.

4.5 Reliability Assessment across Datasets

A trained embedding-and-retrieval system is ideally applicable to any other datasets of images and captions in the same domain. This situation is called a dataset shift (especially a covariate shift). For example, as shown in case (3) in Table 1, the VSE++ trained using the MS COCO dataset works well for the Flickr30k dataset. The samples

have been gathered and annotated in different pipelines, and each dataset has its own bias. An uncertainty measure is expected to have a large average value for samples in a different dataset and in an unknown domain, which can be used to detect the dataset shift [21]. Here, we assess reliability across datasets.

First, we trained VSE++ with VGG19 using the MS COCO training and validation sets. Then, we evaluated it using the test sets of MS COCO, Flickr30k, and RecipeQA datasets [45]. The MS COCO and Flickr30k datasets comprise natural images and their captions, and RecipeQA dataset consists of cooking recipes and corresponding images. Hence, the MS COCO dataset is further from the RecipeQA dataset than the Flickr30k dataset. Each recipe in the RecipeQA dataset is associated with several images. For fair comparison, we randomly chose 1,000 queries and a single target per query.

We plotted the distributions of the uncertainty measures for caption retrieval in Figs. 6 (a) and (b). We set the temperature $T = 0.001$ for the posterior uncertainty but we confirmed that the temperature does not influence the tendency. In Fig. 6 (a), the posterior uncertainty is larger on average for the Flickr30k test set than the MS COCO test set and is much larger for the RecipeQA test set. The posterior uncertainty hence measures the degree of dataset shift. This result indicates that the posterior uncertainty can be a measure of reliability across datasets.

In Fig. 6 (b), the feature uncertainty shows similar distributions for all datasets whereas the performance was highly degraded for Flickr30k dataset (see cases (1) and (3) in Table 1). Moreover, the feature uncertainty of the RecipeQA test set was smaller on average than others. This result is contrary to previously reported results showing that the outputs for unfamiliar samples have large variances [1, 11]. As shown in Section 4.4, the feature uncertainty is large for images depicting many objects even when they are obtained in the same domain. Many images in the RecipeQA depict a few dishes or ingredients and provide smaller feature uncertainty. Hence, the feature uncertainty does not quantify the difference between the MS COCO, Flickr30k, and RecipeQA datasets and does not work as a reliability measure across datasets.

5 CONCLUSION

This study evaluated two uncertainty measures for image-caption embedding-and-retrieval systems implemented using Bayesian deep learning. The feature uncertainty, which is designed by considering the embedding as a regression task, improves the retrieval performance by the model averaging consistently. However, it was found that the feature uncertainty does not assess reliability well in many cases. The posterior uncertainty, which is designed by considering the retrieval as a classification task, successfully assesses the reliability across samples and across datasets. These tendencies were common for different datasets, for different DNN architectures, and for different similarity functions. The qualitative analysis revealed that this difference was caused by the bias in the datasets.

REFERENCES

- [1] Andrei Atanov, Arsenii Ashukha, Dmitry Molchanov, Kirill Neklyudov, and Dmitry Vetrov. 2018. Uncertainty Estimation via Stochastic Batch Normalization. In *International Conference on Learning Representations Workshop (ICLRW)*. arXiv:1802.04893

- [2] David Barber and Christopher M Bishop. 1997. Ensemble Learning for Multi-Layer Networks. In *Advances in Neural Information Processing Systems (NIPS)*.
- [3] Yoshua Bengio. 2012. Deep Learning of Representations for Unsupervised and Transfer Learning. In *ICML Workshop on Unsupervised and Transfer Learning*. 17–36. https://doi.org/10.1007/978-3-642-36657-4_1 arXiv:1305.0445
- [4] Yoshua Bengio, Aaron Courville, and Pascal Vincent. 2013. Representation Learning: A Review and New Perspectives. *IEEE Transactions on Pattern Analysis and Machine Intelligence* 35, 8 (aug 2013), 1798–1828. <https://doi.org/10.1109/TPAMI.2013.50> arXiv:1206.5538
- [5] CM Christopher M CM Bishop. 2006. Pattern recognition and machine learning. In *Springer*, Vol. 4, 738. <https://doi.org/10.1117/1.2819119> arXiv:0-387-31073-8
- [6] Wei-Yu Chen, Yen-Cheng Liu, Zsolt Kira, Yu-Chiang Frank Wang, and Jia-Bin Huang. 2019. A Closer Look at Few-shot Classification. In *International Conference on Learning Representations (ICLR)*.
- [7] Kyunghyun Cho, Bart van Merriënboer, Caglar Gulcehre, Dzmitry Bahdanau, Fethi Bougares, Holger Schwenk, and Yoshua Bengio. 2014. Learning Phrase Representations using RNN Encoder-Decoder for Statistical Machine Translation. In *Conference on Empirical Methods in Natural Language Processing (EMNLP)*. Association for Computational Linguistics, 1724–1734. <https://doi.org/10.3115/v1/D14-1179> arXiv:1406.1078
- [8] Jia Deng, Wei Dong, R. Socher, Li-Jia Li, Kai Li, and Li Fei-Fei. 2009. ImageNet: A large-scale hierarchical image database. In *IEEE Conference on Computer Vision and Pattern Recognition (CVPR)*. IEEE, 248–255. <https://doi.org/10.1109/CVPRW.2009.5206848>
- [9] Fartash Faghri, David J Fleet, Jamie Ryan Kiros, and Sanja Fidler. 2018. VSE++: Improving Visual-Semantic Embeddings with Hard Negatives. In *British Machine Vision Conference (BMVC)*. arXiv:1707.05612
- [10] Andrea Frome, Greg S. Corrado, Jon Shlens, Samy Bengio, Jeff Dean, Marc’Aurelio Ranzato, and Tomas Mikolov. 2013. DeViSE: A Deep Visual-Semantic Embedding Model. *Advances in Neural Information Processing Systems (NIPS)* (2013), 2121–2129. [https://doi.org/10.1016/0921-4534\(95\)00110-7](https://doi.org/10.1016/0921-4534(95)00110-7) arXiv:arXiv:1312.5650v3
- [11] Yarín Gal and Zoubin Ghahramani. 2016. Dropout as a Bayesian Approximation: Representing Model Uncertainty in Deep Learning. In *International Conference on Machine Learning (ICML)*. arXiv:1506.02142
- [12] Yaroslav Ganin and Victor Lempitsky. 2015. Unsupervised Domain Adaptation by Backpropagation. In *International Conference on Machine Learning (ICML)*. 1180–1189. arXiv:1409.7495
- [13] Jiuxiang Gu, Jianfei Cai, Shafiq Joty, Li Niu, and Gang Wang. 2018. Look, Imagine and Match: Improving Textual-Visual Cross-Modal Retrieval with Generative Models. In *IEEE Conference on Computer Vision and Pattern Recognition (CVPR)*. <https://doi.org/10.1109/CVPR.2018.00750> arXiv:1711.06420
- [14] Kaiming He, Xiangyu Zhang, Shaoqing Ren, and Jian Sun. 2016. Deep Residual Learning for Image Recognition. In *IEEE Conference on Computer Vision and Pattern Recognition (CVPR)*. <https://doi.org/10.3389/fpsyg.2013.00124> arXiv:1512.03385
- [15] Matthias Hein, Maksym Andriushchenko, and Julian Bitterwolf. 2019. Why ReLU networks yield high-confidence predictions far away from the training data and how to mitigate the problem. In *IEEE Conference on Computer Vision and Pattern Recognition (CVPR)*. arXiv:1812.05720
- [16] Irina Higgins, Loic Matthey, Arka Pal, Christopher Burgess, Xavier Glorot, Matthew Botvinick, Shakir Mohamed, and Alexander Lerchner. 2017. β -VAE: Learning Basic Visual Concepts with a Constrained Variational Framework. In *International Conference on Learning Representations (ICLR)*. 1–14.
- [17] Geoffrey E. Hinton and Drew van Camp. 1993. Keeping the neural networks simple by minimizing the description length of the weights. In *Annual Conference on Computational Learning Theory (COLT)*. ACM Press, New York, New York, USA, 5–13. <https://doi.org/10.1145/168304.168306> arXiv:1408.5093
- [18] Sergey Ioffe and Christian Szegedy. 2015. Batch Normalization: Accelerating Deep Network Training by Reducing Internal Covariate Shift. In *International Conference on Machine Learning (ICML)*. arXiv:1502.03167
- [19] Himanshu Jain, Yashoteja Prabhu, and Manik Varma. 2016. Extreme Multi-label Loss Functions for Recommendation, Tagging, Ranking & Other Missing Label Applications. In *ACM SIGKDD International Conference on Knowledge Discovery and Data Mining (KDD)*. 935–944. <https://doi.org/10.1145/2939672.2939756>
- [20] Andrej Karpathy and Li Fei-Fei. 2015. Deep visual-semantic alignments for generating image descriptions. In *IEEE Conference on Computer Vision and Pattern Recognition (CVPR)*, Vol. 39. IEEE, 3128–3137. <https://doi.org/10.1109/CVPR.2015.7298932> arXiv:1503.08909v2
- [21] Alex Kendall and Yarín Gal. 2017. What Uncertainties Do We Need in Bayesian Deep Learning for Computer Vision?. In *Advances in Neural Information Processing Systems (NIPS)*. arXiv:1703.04977
- [22] Alex Kendall, Vijay Badrinarayanan, Roberto Cipolla, Vijay Badrinarayanan, and Roberto Cipolla. 2017. Bayesian SegNet: model uncertainty in deep convolutional encoder-decoder architectures for scene understanding. In *British Machine Vision Conference (BMVC)*. arXiv:1511.02680
- [23] Diederik P. Kingma and Jimmy Ba. 2015. Adam: A Method for Stochastic Optimization. In *International Conference on Learning Representations (ICLR)*. 1–15. arXiv:1412.6980
- [24] Diederik P. Kingma and Max Welling. 2014. Auto-Encoding Variational Bayes. In *International Conference on Learning Representations (ICLR)*. 1–14. arXiv:arXiv:1312.6114v10
- [25] Ryan Kiros, Ruslan Salakhutdinov, and Richard S. Zemel. 2014. Unifying Visual-Semantic Embeddings with Multimodal Neural Language Models. 1–13. arXiv:1411.2539
- [26] Armen Der Kiureghian and Ove Ditlevsen. 2009. Aleatory or epistemic? Does it matter? *Structural Safety* 31, 2 (2009), 105–112. <https://doi.org/10.1016/j.strusafe.2008.06.020>
- [27] Christian Leibig and Siegfried Wahl. 2016. Discriminative Bayesian neural networks know what they do not know. In *NIPS Bayesian Deep Learning Workshop*. 1–4.
- [28] Yuncheng Li, Yale Song, and Jiebo Luo. 2017. Improving pairwise ranking for multi-label image classification. In *IEEE Conference on Computer Vision and Pattern Recognition (CVPR)*. 1837–1845. <https://doi.org/10.1109/CVPR.2017.199> arXiv:1704.03135v3
- [29] Tsung Yi Lin, Michael Maire, Serge Belongie, James Hays, Pietro Perona, Deva Ramanan, Piotr Dollár, and C. Lawrence Zitnick. 2014. Microsoft COCO: Common objects in context. In *European Conference on Computer Vision (ECCV)*, Vol. 8693 LNCS. 740–755. https://doi.org/10.1007/978-3-319-10602-1_48 arXiv:1405.0312
- [30] David J. C. MacKay. 1992. A Practical Bayesian Framework for Backpropagation Networks. *Neural Computation* 4, 3 (may 1992), 448–472. <https://doi.org/10.1162/neco.1992.4.3.448>
- [31] Takashi Matsubara, Ryosuke Tachibana, and Kuniaki Uehara. 2018. Anomaly Machine Component Detection by Deep Generative Model with Unregularized Score. In *International Joint Conference on Neural Networks (IJCNN)*.
- [32] Tomas Mikolov, Kai Chen, Greg Corrado, and Jeffrey Dean. 2013. Distributed Representations of Words and Phrases and their Compositionality. In *Advances in Neural Information Processing Systems (NIPS)*, Vol. 1. <https://doi.org/10.1162/jmlr.2003.3.4-5.951> arXiv:1310.4546
- [33] Takeru Miyato, Shin-ichi Maeda, Masanori Koyama, Ken Nakae, and Shin Ishii. 2015. Distributional Smoothing with Virtual Adversarial Training. In *International Conference on Learning Representations (ICLR)*, Vol. 30. 1–18. arXiv:1507.00677
- [34] Anna Rohrbach, Lisa Anne Hendricks, Kaylee Burns, Trevor Darrell, and Kate Saenko. 2018. Object Hallucination in Image Captioning. In *Conference on Empirical Methods in Natural Language Processing (EMNLP)*. arXiv:arXiv:1809.02156v1
- [35] Lorenzo Rosasco, Ernesto De Vito, Andrea Caponnetto, Michele Piana, and Alessandro Verri. 2004. Are Loss Functions All the Same? *Neural Computation* 16, 5 (may 2004), 1063–1076. <https://doi.org/10.1162/089976604773135104>
- [36] Tim Salimans, Ian Goodfellow, Wojciech Zaremba, Vicki Cheung, Alec Radford, Xi Chen, Ishaan Gulrajani, Faruk Ahmed, Martin Arjovsky, Vincent Dumoulin, and Aaron Courville. 2017. Improved Training of Wasserstein GANs. In *Advances in Neural Information Processing Systems (NIPS)*. 1–19. <https://doi.org/10.1109/CVPR.2018.00750> arXiv:1704.00028
- [37] Karen Simonyan and Andrew Zisserman. 2015. Very Deep Convolutional Networks for Large-Scale Image Recognition. In *International Conference on Learning Representations (ICLR)*. 1–14. arXiv:1409.1556
- [38] Lewis Smith and Yarín Gal. 2018. Understanding Measures of Uncertainty for Adversarial Example Detection. *Uncertainty in Artificial Intelligence (UAI)* (2018). <https://doi.org/10.1109/UAI.2018.0000000> arXiv:1803.08533v1
- [39] Nitish Srivastava, Geoffrey E. Hinton, Alex Krizhevsky, Ilya Sutskever, and Ruslan Salakhutdinov. 2014. Dropout: A Simple Way to Prevent Neural Networks from Overfitting. *Journal of Machine Learning Research* 15 (2014), 1929–1958. <https://doi.org/10.1214/12-AOS1000> arXiv:1102.4807
- [40] Ahmed Taha, Yi-Ting Chen, Xitong Yang, Teruhisa Misu, and Larry Davis. 2019. Exploring Uncertainty in Conditional Multi-Modal Retrieval Systems. *arXiv* (2019). arXiv:1901.07702
- [41] Ryo Takahashi, Takashi Matsubara, and Kuniaki Uehara. 2018. RICAP : Random Image Cropping and Patching Data Augmentation for Deep CNNs. In *Asian Conference on Machine Learning (ACML)*.
- [42] Sumio Watanabe. 2010. Equations of states in singular statistical estimation. *Neural Networks* 23, 1 (2010), 20–34. <https://doi.org/10.1016/j.neunet.2009.08.002> arXiv:0712.0653
- [43] Jason Weston, Samy Bengio, and Nicolas Usunier. 2010. Large scale image annotation: Learning to rank with joint word-image embeddings. *European Conference on Machine Learning (ECML)* (2010).
- [44] Yijun Xiao and William Yang Wang. 2019. Quantifying Uncertainties in Natural Language Processing Tasks. *AAAI Conference on Artificial Intelligence (AAAI)* (2019). arXiv:1811.07253
- [45] Semih Yagcioglu, Aykut Erdem, Erkut Erdem, and Nazli Ikizler-Cimbis. 2018. RecipeQA: A Challenge Dataset for Multimodal Comprehension of Cooking Recipes. In *Conference on Empirical Methods in Natural Language Processing (EMNLP)*. arXiv:1809.00812
- [46] M. H. Peter Young, Alice Lai, and J. Hockenmaier. 2014. From image descriptions to visual denotations: New similarity metrics for semantic inference over event descriptions. *Transactions of the Association for Computational Linguistics* 2 (2014), 67–78.

- [47] Hongyi Zhang, Moustapha Cisse, Yann N. Dauphin, and David Lopez-Paz. 2018. mixup: Beyond Empirical Risk Minimization. In *International Conference on Learning Representations (ICLR)*. arXiv:1710.09412
- [48] Li Zhang, Tao Xiang, and Shaogang Gong. 2017. Learning a deep embedding model for zero-shot learning. In *IEEE Conference on Computer Vision and Pattern Recognition (CVPR)*, Vol. 2017-Janua. 3010–3019. <https://doi.org/10.1109/CVPR.2017.321> arXiv:1611.05088
- [49] Quanshi Zhang, Wenguan Wang, and Song-Chun Zhu. 2018. Examining CNN Representations with respect to Dataset Bias. In *AAAI Conference on Artificial Intelligence (AAAI)*. arXiv:1710.10577
- [50] Zhedong Zheng, Liang Zheng, Michael Garrett, Yi Yang, and Yi-Dong Shen. 2017. Dual-Path Convolutional Image-Text Embedding with Instance Loss. *arXiv* 14, 8 (2017), 1–15. arXiv:1711.05535